Proceedings of IECEC'01
36th Intersociety Energy Conversion Engineering Conference
July 29-August 2, 2001, Savannah, Georgia

IECEC2001-TM-15

MODELING HEAT FLOW IN A CALORIMETER EQUIPPED WITH A TEXTURED SOLAR COLLECTOR

Donald A. Jaworske
NASA Glenn Research Center, Cleveland, OH, 44135
Phone: 216-433-2312, FAX: 216-433-2221
e-mail address: Donald.A.Jaworske@grc.nasa.gov

Bradley J. Allen
Ohio State University, Columbus, OH, 44210

ABSTRACT

Heat engines are being considered for generating electric power for minisatellite applications, particularly for those missions in high radiation threat orbits. To achieve this objective, solar energy must be collected and transported to the hot side of the heat engine. A solar collector is needed having the combined properties of high solar absorptance, low infrared emittance, and high thermal conductivity. To test candidate solar collector concepts, a simple calorimeter was designed, manufactured, and installed in a bench top vacuum chamber to measure heat flow. In addition, a finite element analysis model of the collector/calorimeter combination was made to model this heat flow. The model was tuned based on observations from the as-manufactured collector/calorimeter combination. In addition, the model was exercised to examine other collector concepts, properties, and scale up issues.

INTRODUCTION

Heat engines are being considered for use on minisatellites to provide electric power for specific missions, particularly those missions in high radiation threat orbits. Such minisatellites will require a solar collector to absorb incident solar energy, the solar energy must be converted to thermal energy, and the thermal energy must then be transported efficiently to where it is needed. This task must be accomplished with a minimum of radiation loss to the space environment. Hence, a solar collector having the combined properties of high solar absorptance, low infrared emittance, and high thermal conductivity will be needed to collect solar energy and transport the energy to the hot side of the heat engine, envisioned to be between 500 and 750 K. Candidate high thermal conductivity substrates for the solar collector may include composites made from high thermal conductivity pitch based graphite fibers or high thermal conductivity thermopyrolytic graphite sandwiched between two face sheets of aluminum. Candidate surface finishes and coatings for the solar collector may include textured features [1], cermet composite coatings [2,3], or multilayer thin film coatings [4].

One way to evaluate the successful performance of a prospective solar collector and to evaluate the effectiveness of the solar collector's combined properties is to identify the heat flow collected and transported by the collector utilizing a calorimeter. An Inconel 718 calorimeter was designed, built, and installed in a vacuum chamber equipped with a light source to accomplish this task. Simulated sunlight impinging on the solar collector is absorbed and transported to the top of

a 2.54 cm diameter Inconel 718 rod. Water cooling extracts heat at the base of the rod. Heat flowing through the rod is measured using two thermocouples separated by a known distance. Four solar collectors were manufactured for use with the calorimeter, three identical textured graphite solar collectors and one aluminum solar collector.

Another way to evaluate the performance of many prospective solar collectors is to identify heat flow utilizing a finite element analysis model. A finite element analysis model was developed using the known geometry of the solar collectors and the Inconel 718 calorimeter. The model was calibrated with the known properties of the four solar collectors. Exercising the model under different conditions yielded information about other potential solar collector concepts.

This paper summarizes the heat flow measured by an Inconel 718 calorimeter as-captured by either a textured graphite solar collector or a mirror-like aluminum solar collector. The performance of the solar collectors was evaluated over several operating conditions. This paper also summarizes the finite element analysis model used to simulate the calorimeter performance and the results of exercising that model over various conditions.

MATERIALS AND METHODS

Inconel 718 was selected as the material of choice for the calorimenter for two reasons. The thermal conductivity of Inconel 718 is well known and Inconel 718 is often used to manufacture the hot side of a Stirling heat engine [5]. Hence, the solar collector ultimately chosen for use is likely to be connected to an Inconel 718 heater head.

Three essentially identical solar collectors were manufactured for this study, all made from chopped pitch based K-1100 graphite fibers embedded in an RS-3 isocyanate ester matrix. The part was manufactured by CCS Composites, Benicia, CA using a proprietary injection molding process. The surface to-be-exposed to the simulated sunlight was textured in a directed atomic oxygen beam at NASA Glenn Research Center to yield a surface having a high solar absorptance and a moderate infrared emittance [1]. Coupons of similar textured K-1100/RS-3 composites were evaluated optically and had a solar absorptance of 0.947 and an infrared emittance of 0.808.

A fourth solar collector was manufactured for this study, made from aluminum. This part was manufactured at NASA Glenn Research Center and the surface to-be-exposed to the simulated sunlight was diamond turned to a mirror-like finish. The mirror-like finish had a low solar absorptance of 0.106, and a low infrared emittance of 0.121.

The shape of all four solar collectors was identical. The overall diameter of 7.62 cm was selected owing to the size limitations imposed by the supporting hardware (i.e. the solar simulator beam diameter and the glass window installed in the vacuum chamber). The solar collectors were tapered, to accommodate a conical interface with the Inconel 718 calorimeter. A conical interface was selected so that the solar collector could be placed on top of the Inconel 718 calorimeter under slight compression, by tightening a polished aluminum cap screw. This design also allowed easy exchange of one solar collector with another.

The thermal energy collected by the solar collector enters at the top of the Inconel 718 rod and exits at the bottom of the rod. A temperature gradient is established within the rod. Temperatures at two locations are detected by thermocouples placed a known distance apart. The thermocouple holes were drilled such that the two thermocouples could be potted at or near the center of the Inconel 718 rod. Care was taken to wrap the thermocouple wire around the Inconel 718 rod to minimize heat loss down the wire. The finish on the Inconel 718 was bright, and had an emittance of 0.139. A schematic diagram of the solar collector and calorimeter design is shown in Figure 1.

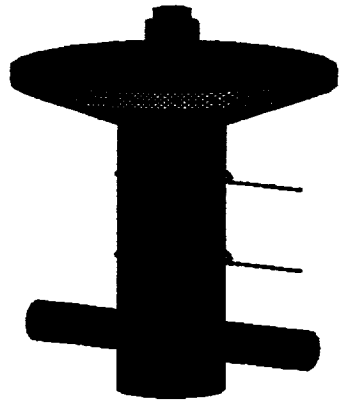

Figure 1. Schematic diagram of the solar collector calorimeter combination.

A bench top vacuum chamber was utilized to house the solar collector and calorimeter combination. The chamber was equipped with a small turbomolecular pump backed by a roughing pump and could achieve a vacuum of approximately 40 millitorr, to minimize the effects of convection. Chilled water from a closed-loop water cooling system was introduced to the chamber through matching feedthroughs. The temperature selected for water cooling was 290 K.

Other feedthroughs provided access to the type T thermocouples. A Keithley model 740 System Scanning Thermometer was used to capture the temperature data. The Keithley 740 was connected to a portable computer via an IEEE-488 communications bus, to accomodate the exchange of control commands and data. A computer program was used to store the temperature data as a function of time.

Simulated solar energy was delivered to the chamber utilizing a 1000 watt quartz halogen light source. The output beam of the solar simulator was measured at four different power settings utilizing a calibrated radiometer. These four power settings were used throughout solar collector testing. In practice, the output of the beam was allowed to pass into the vacuum chamber through a 10.16 cm diameter window. The intensity of the four power settings is summarized in Table I.

Table I. Intensity of solar simulator.

Power Setting (volts)		Intensity (W/cm^2)
30		0.0302
40		0.0765
50		0.1176
60		0.1510

The steady state finite element analysis model developed here was based on the geometry of the as-manufactured collector and calorimeter. The finite element analysis model was assembled using the TAK II thermal analysis kit, K&K Associates, Westminster, CO. Most of the energy entering the system was absorbed by the front face of the solar collector. A provision was made to allow some energy (0.3395 of incident energy) to be absorbed on the back side of the solar collector to take into account those rays that bounced off the stainless steel chamber walls. In a space application, this provision could be zeroed out, or lessened based on reflections from the spacecraft.

The water cooling was modeled utilizing a boundary node of infinite capacitance, a fair assumption given the capacity of the closed loop water cooling system. Other details of the computer model included various parameters collected through laboratory measurements or literature values. Table II summarizes all the physical properties utilized by the model.

Matching model performance with the performance of the as-manufactured calorimeter was accomplished by matching the temperatures of two specific nodes with the temperatures of the two thermocouples. The location of the nodes coincided with the location of the thermocouples. Temperature data at steady state were used for comparison. An iterative process was used to calibrate the model, by making small changes in such parameters as the energy absorption on the back side of the solar collector and the correction factor used to account for the loss of energy through the vacuum chamber window. These changes were made to bring the temperatures of the model into agreement with the observed thermocouple readings, at all four power settings.

Table II Optical and Physical Properties Utilized for Modeling.

Property	Value	Comments
Absorptance of Textured Graphite	0.947	Measured
Emittance of Textured Graphite	0.808	Measured
Absorptance of Aluminum	0.106	Measured
Emittance of Aluminum	0.121	Measured
Emittance of Inconel 718	0.139	Measured
Density of Composite	1.77 g/cm^3	Measured
Density of Aluminum	2.70 g/cm^3	Reference 6
Density of Inconel 718	8.25 g/cm^3	Reference 6
Heat Capacity of Composite	0.69 Ws/gK	Estimated
Heat Capacity of Aluminum	0.90 Ws/gK	Reference 6
Heat Capacity of Inconel 718	0.445 Ws/gK	Reference 6
Thermal Conductivity of Composite	0.886 W/cmK	Estimated
Thermal Conductivity of Aluminum	2.09 W/cmK	Reference 6
Thermal Conductivity of Inconel 718	0.111 W/cmK	NIST
Temperature of Vacuum Chamber Wall	300 K	Estimated

RESULTS AND DISCUSSION

Figure 2 summarizes the actual thermocouple temperatures obtained utilizing the three textured graphite solar collectors and the fourth aluminum solar collector. Steady state

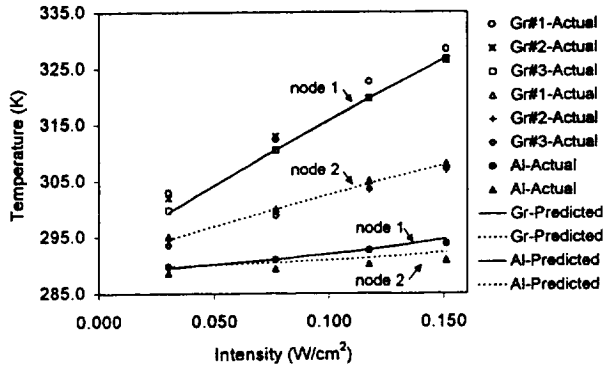

Figure 2. Predicted and observed thermocouple temperatures used to calculate heat flow.

temperatures were obtained at all four power settings. The modeling results for the thermocouple nodes from the calibrated model are also shown. Node 1 represents the thermocouple nearest to the heat source, while node 2 represents the thermocouple nearest to the water cooling.

The heat flow can also be summarized graphically at all four power settings, for the three textured graphite solar collectors and the aluminum solar collector, as well as the heat flow predictions provided by the model. Figure 3 summarizes the actual and predicted heat flow through the Inconel 718 calorimeter, in watts. The model predicts the thermocouple temperatures quite well, however it tends to underestimate heat flow.

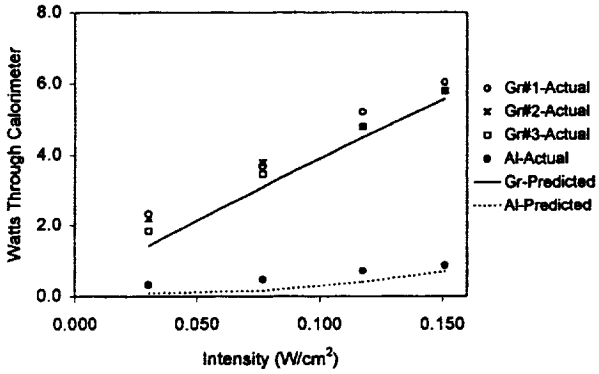

Figure 3. Predicted and observed heat flow in the Inconel 718 calorimeter.

Comparative Modeling

A total of four different solar intensities were used to illuminate the solar collector, yielding four different steady state conditions within the calorimeter. The range of solar intensities purposely encompass the value of the air mass zero solar constant, 1.37 W/cm^2. As expected, the textured graphite solar collector yielded a greater overall temperature, a greater temperature difference between the thermocouples, and a greater heat flow compared to the polished aluminum collector. This was expected owing to the much greater solar absorptance of the textured graphite compared to the polished aluminum.

Radiant energy leaving the system is received by the stainless steel walls of the vacuum chamber, at or near room temperature. A cold wall was not available to simulate the space environment. Hence, the radiant energy leaving the system in practice is considered to be less than would otherwise be observed in the space environment.

Under maximum illumination, estimated to be slightly greater than the air mass zero solar constant, the model predicts the temperature of the textured graphite solar collector to be 351 K. Figure 4a summarizes the heat flow under this condition and shows 8.89 watts entering the solar collector, 6.91 watts from direct illumination and 1.98 watts from reflections. Figure 4a also shows 5.56 watts of energy leaving the system through water cooling. The balance of the energy leaving the system is through radiant heat transfer, mostly from the solar collector. A negligible amount of energy is leaving the system through the sides of the Inconel 718 calorimeter.

The model predicts the temperature of the polished aluminum solar collector to be 298 K. Figure 4b shows 1.00 watt entering the solar collector, 0.78 watts from direct illumination and 0.22 watts from reflections. Figure 4b also shows 0.72 watts of energy leaving the system through water cooling. Again, the balance of the energy leaving the system is through radiant heat transfer.

Predictive Modeling

Once a model is available, it is possible to vary different parameters in the model to see how overall performance varies. Exercising the model in this way helps predict potential performance under conditions that have not been specifically studied in the laboratory. It also provides guidance on where future effort should be placed.

The range of potential values for modeling was selected based on optical properties that could be found in the literature, potential solar intensities from solar concentrators, candidate solar collector radii, and the likely temperature of a cold wall.

In space, the solar collector will operate in a thermal environment yielding greater radiant heat transfer than available laboratory conditions allow. A sink temperature of

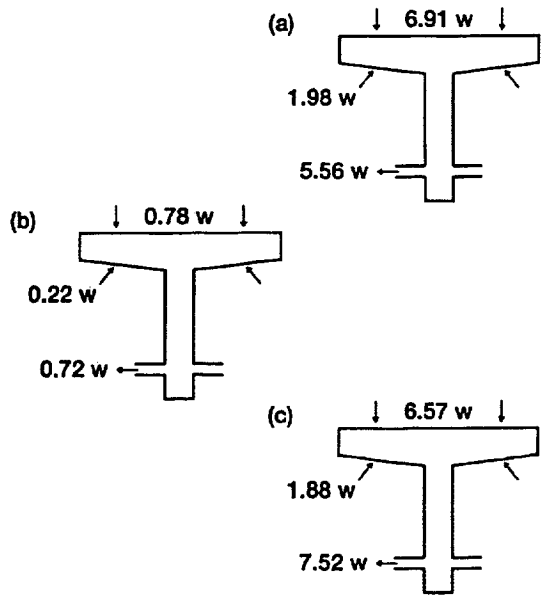

Figure 4. Heat flow in the calorimeter using a) the textured graphite solar collector and b) the mirror-like aluminum solar collector, and c) heat flow predicted by modeling.

80 K simulating liquid nitrogen cooled cold walls was prescribed in the model to simulate the space environment.

Exercising the model using variations of the parameters allows prediction of performance under differing conditions. Varying optical properties, solar intensity, and collector size serve to predict the performance of the solar collector when using other materials of construction or when using different solar intensities or collection areas.

Figure 4c summarizes the energy flow in a system where the values of 0.90 and 0.03 are used for solar absorptance and infrared emittance, respectively. In addition, 80 K is imposed on the chamber wall boundary condition. Substituting these values into the model yields 8.45 watts entering the system. Of the energy entering the system, 7.52 watts pass through the calorimeter. The balance is rejected to the surroundings, held at 80 K in this case.

Another way to enhance total energy entering the calorimeter is to utilize a primary concentrator to increase the solar flux impinging on the solar collector. Concentration factors vary depending on the size and type of concentrator. For this study, a modest concentration factor between 1 and 4 is applied to the model. Figure 5 summarizes the results obtained when exercising the model over this concentration factor range, utilizing solar absorptance and infrared emittance values of 0.90 and 0.03, respectively. The temperature of the solar collector under these conditions gets as high as 626 K and the heat passing through the calorimeter increases to 30.3 watts . Along with the higher temperature goes the assumptions that the optical coating will remain intact and that the optical properties will remain unchanged. (Unfortunately, the model does not accommodate changes in the optical properties as a function of temperature. Emittance, for example, will most certainly increase with increasing temperature.) Other items that factor into utilizing a concentrator include pointing and tracking concerns and durability of the concentrator in the space environment.

The next area of concern is scaling. Figure 5 also summarizes the impact of solar collector size on the energy collected by the prospective solar collector. Doubling the radius quadruples the area of the solar collector, increasing the solar collector temperature to 550 K and increasing the heat passing through the calorimeter to 23.2 watts. (Again, the model does not accommodate changes in the optical properties as a function of temperature.) Scaling to a larger solar collector may be more practical than the approach of using a concentrator, owing to its simplicity. Additional scaling should yield additional enhancements in performance until the thermal properties of the solar collector become limiting.

Increasing solar collection area, by way of concentration or by way of increased surface area, yields a substantial increase in the temperature of the solar collector. In such a case, an organic based composite would be unacceptable. An inorganic solar collector substrate should be used.

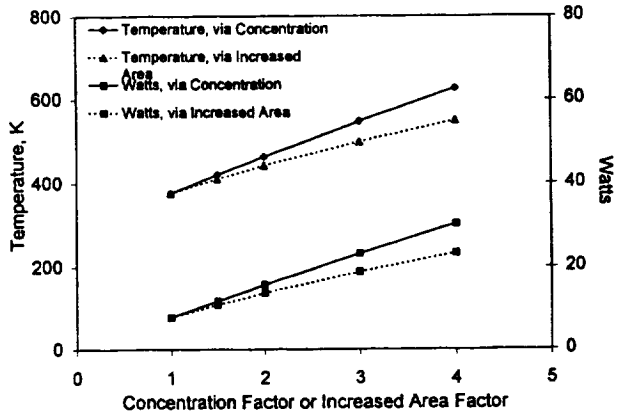

Figure 5. Solar collector performance as a function of concentration factor or area.

FUTURE WORK

The modeling suggests that the direction of future work should be in three areas: utilize a graded coating or a metal-dielectric cermet coating to achieve attractive optical properties, increase the collection area, and increase the temperature capability of the solar collector. These items must be addressed in concert, without interfering with the high thermal conductivity of the substrate. The melting point of aluminum is 660°C and inorganic coatings on an aluminum face sheet may be entirely acceptable. Encapsulated thermopyrolytic graphite could be used to enhance the thermal conductivity of the aluminum.

CONCLUSIONS

Small heat engines are being considered for use on minisatellites. Solar collectors having the combined properties of high solar absorptance, low infrared emittance, and high thermal conductivity must be developed to supply energy to the small heat engines. Four candidate solar collectors were designed and manufactured, three identical graphite fiber isocynate ester composites that were textured in a directed atomic oxygen beam and an aluminum solar collector diamond turned to a mirror-like finish. In addition, an Inconel 718 calorimeter was designed and manufactured to measure heat flow. Heat flow in the calorimeter was evaluated for each solar collector, utilizing simulated sunlight entering a bench top vacuum chamber. In addition, a finite element analysis model was developed to model the performance of the solar collector Inconel 718 calorimeter combination. The model was in good agreement with observed temperatures and heat flow, and was further utilized to predict solar collector performance under conditions not specifically studied in the laboratory. Modeling results suggest that the solar collector can be scaled to the desired temperature and energy throughput needed for heat engine applications, however, additional work is needed to develop a cermet coating that can be applied to a solar collector composed of thermopyrolytic graphite sandwiched between two aluminum face sheets.

ACKNOWLEDGMENTS

The authors gratefully acknowledge Mr. Edward A. Sechkar, Dynacs Inc., for his help in designing the calorimeter and all of the supporting hardware.

REFERENCES

1. Banks, B. A., Rutledge, S. K, Paulsen, P. E., and Steuber, T. J., 1989, "Simulation of the Low Earth Orbital Atomic Oxygen Interaction With Materials by Means of an Oxygen Ion Beam," NASA Technical Memorandum 101971.
2. Granqvist, C. G., 1991, "Solar Energy Materials, Overview and Some Examples, " Appl. Phys. A, Vol. 52, pp. 83-93.
3. Zhang, Q., Zhao, K., Zhang, B.-C., Wang, L.-F., Shen, Z.-L., Lu, D.-Q., Xie, D.-L., and Li, B.-F., 1999, "High Performance Al-N Cermet Solar Coatings Deposited by a Cylindrical Direct Current Magnetron Sputter Coater," J. Vac. Sci. Tech. A, Vol. 17 (5), pp 2885-2890.
4. Adsten, M., Joerger, R., Jarrendahl, K., and Wackelgard, E., 2000, "Optical Characterization of Industrially Sputtered Nickel-Nickel Oxide Solar Selective Surface," Solar Energy, Vol. 68 (4), pp 325-328.
5. Personal Communication, February, 2000, Stirling Technology Company, Kennewick, WA.
6. Perry, R. H., and Chilton, C. H., 1973, Chemical Engineers' Handbook, 5th Edition, McGraw-Hill Book Company, New York.